Interfaces of semi-infinite smectic liquid crystals and equations of state of infinite smectic stacks of semiflexible manifolds

Lianghui Gao and Leonardo Golubović
Physics Department, West Virginia University, Morgantown, West Virginia 26506-6315
(Received 15 October 2002; published 27 February 2003)

In this paper, we first elucidate the classical problem of the elastic free energy of a semi-infinite smectic-*A* liquid crystals, that fills the semispace above an interface (a boundary smectic layer) of a given shape. For the free energy of this interface, we obtain an effective interface Hamiltonian that takes into account the system discreteness introduced by the layered character of smectic-*A* liquid crystals. It is thus applicable to both short and long wavelength fluctuations of the interface shape. Next, we use our interface Hamiltonian to develop an efficient approach to the statistical mechanics of stacks of *N* semiflexible manifolds, such as two-dimensional smectic phases of long semiflexible polymers and three-dimensional lamellar fluid membrane phases. Within our approach, doing the practically interesting thermodynamic limit $N\to\infty$ is reduced to considering a small stack, with just a few interacting manifolds, representing a subsystem of an infinite smectic. This dramatic reduction in the number of degrees of freedom is achieved by treating the first (the last) manifold of the small stack as an interface with the semi-infinite smectic medium below (above) the small stack. We illustrate our approach by considering in detail two-dimensional sterically stabilized smectic liquid crystals of long semiflexible polymers with hard-core repulsion. Smectic bulk ($N=\infty$) equation of state and the universal constant characterizing entropic repulsion in these phases are obtained with a high accuracy from numerical simulations of small subsystems with just a few semiflexible polymers.

DOI: 10.1103/PhysRevE.67.021708 PACS number(s): 61.30.Jf, 87.15.−v, 82.70.Kj

I. INTRODUCTION

Substantial effects of thermal fluctuations keep smectic liquid crystals and smecticlike phases in the focus of theoretical and experimental statistical physics [1–8]. The most recent investigations of the fundamental properties of smectics are related to structural and thermodynamic properties of two-dimensional (2D) smectic-*A* phases [1,2]. They have been stimulated by recent discovery of such a phase of long DNA molecules intercalated between lipid membranes in DNA-cationic-lipid complexes [3–8]. In these systems, long semiflexible DNA molecules themselves form stacks of one-dimensional smectic layers that are low-dimensional analogs of lamellar fluid membrane phases and other three-dimensional smectic-*A* phases [9–15]. In smectic liquid crystals, thermal fluctuations affect material properties over a broad range of length scales. Thus, the long length scale fluctuations (with wavelength typically much larger than the smectic phase period a), destroy true long-range positional order of smectic layers [1,14,15], and induce the anomalous elastic behavior in both 2D and 3D smectic liquid crystals [2,16]. On the other side, shorter, mesoscopic length scale fluctuations may have significant effects on basic smectic properties such as the equation of state. Typical examples for this are sterically stabilized smectic phases of large flexible manifolds, such as the stacks of long semiflexible polymers or fluid membranes interacting with purely hard-core repulsion [9–13]. In these lyotropic smectic liquid crystals, elastic constants and the smectic equation of state, that relates the isotropic osmotic pressure P to the smectic period a, are purely entropic in origin [9–11,17–23]. These properties are dominated by strong fluctuations of thermally rough flexible manifolds forming smectic stacks.

Similar entropic effects may be significant also in smectic systems, in which the interactions between flexible manifolds are not purely steric. Smectic elastic constants, equation of state, etc., result from a subtle interplay between entropic effects and various microscopic (bare) interactions between flexible manifolds. Finding basic material properties of smectic stacks of *N* interacting flexible manifolds is, generally, a difficult statistical mechanics problem, especially in the experimentally interesting thermodynamic limit $N\to\infty$ needed to obtain the bulk properties of these phases.

In this paper, we attack this complex multimanifold problem by relating it to another interesting problem of the physics of smectic liquid crystals. It is the classical problem of the elastic energy of *semi-infinite* smectic-*A* liquid crystal that fills the semispace above a boundary smectic layer (interface) of a given shape [15]. In the continuum limit, as discussed by de Gennes and Prost [15], free energy of this semi-infinite smectic liquid crystal is given by an effective interface Hamiltonian, with a suitably defined interfacial tension

$$\delta\gamma=\sqrt{K_{sm}B_{sm}}. \tag{1.1}$$

Here, K_{sm} and B_{sm}, are, respectively, smectic bending and compressibility elastic moduli. $K_{sm}=\kappa/a$, for a stack of flexible manifolds with bending rigidity κ, that forms a smectic liquid crystal with the period a. In this paper, we first generalize this standard continuous smectic interface Hamiltonian by taking into account the system discreteness due to the layered character of smectic liquid crystals, as detailed in Sec. II. Therein, we obtain an effective interface free energy functional applicable to both short and long wavelength fluc-

tuations of the interface shape. It has the form, for the d-dimensional interfaces of $(d+1)$-dimensional smectic-A liquid crystals,

$$H_{int}=\frac{1}{2}\int \frac{d^d\mathbf{q}}{(2\pi)^d}K_{semi}(q)|\tilde{h}(\mathbf{q})|^2. \tag{1.2}$$

Here, $\tilde{h}(\mathbf{q})$ is the Fourier transform of the interface profile ($q=|\mathbf{q}|$), whereas $K_{semi}(q)$ is the dispersion relation giving the free energy cost associated with the interface fluctuations with the wave vector q. The detailed form of $K_{semi}(q)$ is discussed in Sec. II, see Eq. (2.16) therein. For small q, $K_{semi}(q)\approx\delta\gamma q^2$, and our dispersion relation reduces to that of the simple interface model, with interfacial tension $\delta\gamma$ in Eq. (1.1), discussed in the classical liquid crystal discussion of de Gennes and Prost [15]. On the other side, for large q, $K_{semi}(q)\approx\kappa q^4$, corresponding to the bending elastic behavior of a free manifold. In between these two extreme limits, the actual interface fluctuation energy cost is governed by a more complex dispersion relation derived and discussed in Sec. II.

We use our interface Hamiltonian in Sec. III, to develop an efficient approach to the statistical mechanics of the stacks of N d-dimensional flexible manifolds, such as two-dimensional smectic phases of long semiflexible polymers ($d=1$) and three-dimensional lamellar phases of fluid membranes ($d=2$). Within our approach, doing the practically interesting thermodynamic limit $N\to\infty$ is reduced to considering a *small stack* (with a few interacting manifolds) that is a *subsystem* of an infinite smectic stack. Such a dramatic reduction in the number of degrees of freedom is achieved by treating the first (the last) manifold of the small stack as an interface with the semi-infinite smectic medium below (above) the small stack. The effective free energy of these interface manifolds is as in Eq. (1.2). Within our approach to infinite smectic liquid crystals, the dispersion relation in Eq. (1.2) takes into account the manifolds in the semi-infinite media that are above and below the small stack representing a subsystem of an infinite smectic. By the use of Eq. (1.2), the manifolds in the two semi-infinite media are effectively integrated out of the infinite system partition function, very much in the spirit of effective Hamiltonians employed (in a different way) in the renormalization group theories [24]. Thus, the difficult statistical mechanics problem with an infinite number of manifolds is reduced to a tractable problem of a small stack with just few manifolds, as detailed in Sec. III.

Our approach to infinite smectic stacks is illustrated here by considering in detail sterically stabilized two-dimensional smectic phases of long semiflexible polymers with hard-core repulsion (Sec. IV). Thanks to the aforementioned character of our approach, the equation of state and universal constants characterizing entropic elasticity in these phases are obtained, with a high accuracy, already from Monte Carlo simulations of small stacks with just a few polymers.

This paper is organized as follows: In Sec. II, we discuss the surface free energy of semi-infinite smectic-A liquid crystals, and derive our interfacial Hamiltonian. In Sec. III, we incorporate the results of Sec. II into our theory of small subsystems of infinite smectic stacks. In Sec. IV, we apply our approach to investigate, by Monte Carlo simulations, the sterically stabilized 2D smectic liquid crystals comprised of long semiflexible polymers. We summarize our findings in Sec. V. Appendix A illuminates the discussion of Sec. II from a different point of view. Also, therein and in Appendix B, we discuss a few substantial details of our simulations.

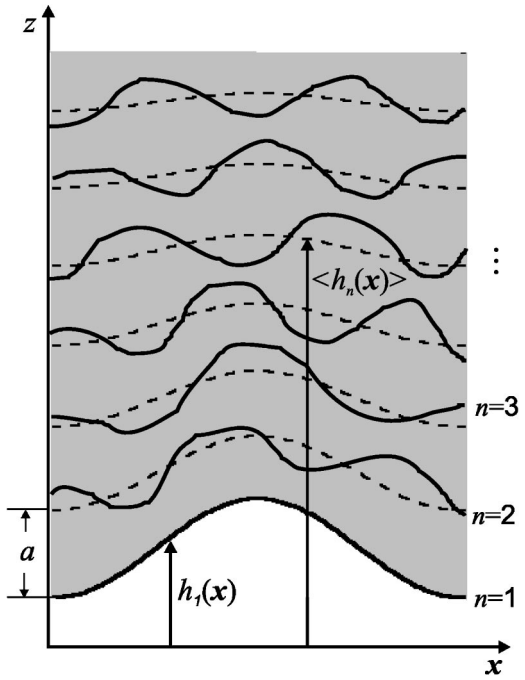

FIG. 1. A semi-infinite smectic stack of manifolds over the manifold with the height function $h_1(\mathbf{x})$ at the boundary (interface) of the stack. By the use of the effective interface model for $h_1(\mathbf{x})$ in Eqs. (2.23) and (2.24), the manifolds in the smectic medium above the interface, with $n=2,3,\ldots,$ are integrated out of the system's partition function. Instantanous configurations of the manifolds are given by the solid lines. For a *given* $h_1(\mathbf{x})$, the manifolds fluctuate around the average positions $\langle h_n(\mathbf{x})\rangle$ indicated by dashed lines.

II. SEMI-INFINITE SMECTIC-*A* LIQUID CRYSTALS OVER BOUNDARY OF A GIVEN SHAPE

In this section we address the classical problem of the elastic free energy of a semi-infinite smectic-A liquid crystal that fills the semispace above a boundary smectic layer (interface) of a given shape [15], see Fig. 1. For the free energy of this interface, we derive here an effective interface Hamiltonian that takes into account the system discreteness due to layered nature of smectic-A liquid crystals. We thus obtain an interface model applicable to both short and long wavelength fluctuations of the interface shape, see Eqs. (2.15) and (2.16) in the following.

To discuss semi-infinite smectic liquid crystals, we consider a smectic stack of N d-dimesional flexible manifolds (with bending rigidity κ), each described by its height function $h_n(\mathbf{x})$ above d-dimensional $\mathbf{x}$ plane (base plane), $n=1,2,\ldots,N$. The effective free energy functional of this $(d+1)$-dimensional smectic system at constant isotropic

pressure P has the form [8,23],

$$H_{eff}(\{h_n\}) = \int d^d\mathbf{x}\Bigg[P[h_N(\mathbf{x}) - h_1(\mathbf{x})] + \sum_{n=1}^{N-1} V_{eff}(h_{n+1}(\mathbf{x}) - h_n(\mathbf{x})) + \sum_{n=1}^{N} \frac{\kappa}{2}\left(\frac{\partial^2 h_n(\mathbf{x})}{\partial \mathbf{x}^2}\right)^2\Bigg]. \tag{2.1}$$

Here, P is the isotropic osmotic pressure exerted on the stack, whereas V_{eff} is the *effective* intermanifold interaction potential [23]. V_{eff} takes into account entropic effects of manifold fluctuations [23]. Minimization of the effective free energy functional in Eq. (2.1) can be used to investigate nonuniform smectic configurations induced, for example, by external forces displacing system boundaries [8]. In the absence of such forces, minimizing Eq. (2.1), with the uniform $h_{n+1}(\mathbf{x}) - h_n(\mathbf{x}) = a$, yields the equilibrium smectic equation of state

$$P = -\frac{\partial V_{eff}(a)}{\partial a}, \tag{2.2}$$

determining, with appropriately defined $V_{eff}(a)$, the smectic phase period a for a given osmotic pressure P [23]. To investigate spatially nonuniform equilibrium configurations of the smectic stack, we expand Eq. (2.1) around its minimum to obtain the harmonic smectic elastic Hamiltonian

$$H_{el} = \int d^d\mathbf{x}\Bigg[a\sum_{n=1}^{N-1} \frac{B_{sm}}{2}\left(\frac{h_{n+1}(\mathbf{x}) - h_n(\mathbf{x}) - a}{a}\right)^2 + a\sum_{n=1}^{N} \frac{K_{sm}}{2}\left(\frac{\partial^2 h_n(\mathbf{x})}{\partial \mathbf{x}^2}\right)^2\Bigg], \tag{2.3}$$

where

$$K_{sm} = \frac{\kappa}{a} \tag{2.4}$$

is the smectic bending modulus, and

$$B_{sm} = -a\frac{\partial P(a)}{\partial a} = a\frac{\partial^2 V_{eff}(a)}{\partial a^2}, \tag{2.5}$$

is the true (renormalized) smectic compressibility [23]. Equation (2.3), with $N=\infty$, can be directly used to find the free energy of semi-infinite smectic stack in the situations in which the first member of the stack ($n=1$) has a *given* shape $h_1(\mathbf{x})$, see Fig. 1. For that purpose, we introduce, into Eq. (2.3), the smectic phonon variables $u_n(\mathbf{x})$, via

$$h_n(\mathbf{x}) = u_n(\mathbf{x}) + (n-1)a, \tag{2.6}$$

and minimize the discrete smectic Hamiltonian (2.3) over $u_2(\mathbf{x})$, $u_3(\mathbf{x})$, . . . , for a *fixed* form of $u_1(\mathbf{x}) \equiv h_1(\mathbf{x})$ to obtain

$$0 = -B_{sm}\frac{u_{n+1}(\mathbf{x}) - 2u_n(\mathbf{x}) + u_{n-1}(\mathbf{x})}{a^2} + K_{sm}\left(\frac{\partial^2}{\partial \mathbf{x}^2}\right)^2 u_n(\mathbf{x}) \tag{2.7}$$

for $n = 2,3, \ldots$. Solving Eq. (2.7) yields the *average* positions of smectic layers $\langle h_n(\mathbf{x})\rangle = (n-1)a + u_n(\mathbf{x})$, $n = 2,3, \ldots$, for a given shape of the interfacial manifold, $h_1(\mathbf{x}) = u_1(\mathbf{x})$, see Fig. 1. To solve Eq. (2.7), we introduce the partial Fourier transform,

$$u_n(\mathbf{x}) = \int \frac{d^d\mathbf{q}}{(2\pi)^d} e^{i\mathbf{q}\cdot\mathbf{x}}\tilde{u}_n(\mathbf{q}), \tag{2.8}$$

reducing Eq. (2.7) to the difference equation

$$0 = -B_{sm}\frac{\tilde{u}_{n+1}(\mathbf{q}) - 2\tilde{u}_n(\mathbf{q}) + \tilde{u}_{n-1}(\mathbf{q})}{a^2} + K_{sm}q^4\tilde{u}_n(\mathbf{q}), \tag{2.9}$$

($q = |\mathbf{q}|$). We need the solution to Eq. (2.9) satisfying the boundary conditions: $u_n \to 0$ for $n \to \infty$, and $u_1 = h_1$, the given shape of the $n=1$ manifold in the stack, see Fig. 1. It has the form

$$\tilde{u}_n(\mathbf{q}) = [R(q)]^{n-1}\tilde{h}_1(\mathbf{q}). \tag{2.10}$$

By Eqs. (2.9) and (2.10),

$$R(q) - 2 + \frac{1}{R(q)} = a^2\lambda^2 q^4, \tag{2.11}$$

where

$$\lambda = \sqrt{\frac{K_{sm}}{B_{sm}}} = \sqrt{\frac{\kappa}{-a^2\dfrac{\partial P(a)}{\partial a}}} \tag{2.12}$$

is the de Gennes penetration length of the smectic stack. As $u_n \to 0$ for $n \to \infty$, we need the solution to Eq. (2.11) which is less than 1. It is easily found to be

$$R(q) = 1 + \frac{1}{2}a^2\lambda^2 q^4 - \sqrt{a^2\lambda^2 q^4 + \left(\frac{a^2\lambda^2 q^4}{2}\right)^2}. \tag{2.13}$$

The system's free energy Eq. (2.3) can be, by Eqs. (2.6) and (2.8), expressed as

$$H_{el} = \int \frac{d^d\mathbf{q}}{(2\pi)^d} a\sum_{n=1}^{\infty}\left[\frac{B_{sm}}{2}\left|\frac{\tilde{u}_{n+1}(\mathbf{q}) - \tilde{u}_n(\mathbf{q})}{a^2}\right|^2 + \frac{K_{sm}}{2}q^4|\tilde{u}_n(\mathbf{q})|^2\right] \tag{2.14}$$

in terms of the partial Fourier transform variables $\tilde{u}_n(\mathbf{q})$. By inserting, into Eq. (2.14), $\tilde{u}_n(\mathbf{q})$ given by Eqs. (2.10) and (2.13), we find, by a straightforward calculation, the form of the interface Hamiltonian

$$H_{int} \equiv H_{el} = \frac{1}{2} \int \frac{d^d \mathbf{q}}{(2\pi)^d} K_{semi}(q) |\tilde{h}_1(\mathbf{q})|^2 \qquad (2.15)$$

with

$$K_{semi}(q) = \sqrt{(\delta\gamma q^2)^2 + \left(\frac{\kappa q^4}{2}\right)^2} + \frac{\kappa q^4}{2}. \qquad (2.16)$$

Here,

$$\delta\gamma = \sqrt{K_{sm} B_{sm}} = B_{sm} \lambda \qquad (2.17)$$

is the ''surface tension'' noted in previous studies [8,15]. By Eqs. (2.4) and (2.5), $\delta\gamma$ can be expressed also as

$$\delta\gamma = \sqrt{-\kappa \frac{\partial P(a)}{\partial a}} \qquad (2.18)$$

in terms of the quantities more appropriate for the smectic stacks of manifolds.

We comment on the physical aspects of our interface model in Eqs. (2.15) through (2.18): First, as usual, the interface dispersion relation $K_{semi}(q)$ in Eq. (2.16) vanishes at $q=0$. This must be the case, as the uniform configuration of the boundary manifold, $h_1(\mathbf{x}) = \text{const}$, corresponds to a simple translation of the whole stack and thus costs no energy. Next, note that the form of $K_{semi}(q)$ suggests the characteristic length scale L_b (i.e., momentum scale q_b), defined by

$$L_b = \frac{1}{q_b} = \sqrt{\frac{\kappa}{\delta\gamma}} = \sqrt{a\lambda} \qquad (2.19)$$

the ''healing length,'' encountered in previous studies (see Ref. [8]). At this (momentum) scale, the two terms under the square root in Eq. (2.16) balance. By Eq. (2.18), L_b can be expressed also as

$$L_b = \left(\frac{\kappa}{-\frac{\partial P(a)}{\partial a}} \right)^{1/4} \qquad (2.20)$$

in terms more appropriate for smectic stacks of manifolds. By Eq. (2.16), one recovers the two characteristic behaviors:

(i) For $q \ll q_b$, by expanding Eq. (2.16),

$$K_{semi}(q) = \delta\gamma\, q^2 + O(q^4) \qquad (2.21)$$

corresponding to interfaces with the surface tension $= \delta\gamma$. In this long length scale limit, our interface model reduces to the standard smectic interface model [8,15].

(ii) For $q \gg q_b$, by expanding Eq. (2.16) rewritten as

$$K_{semi}(q) = \frac{1}{2}\, \kappa q^4 \left[\sqrt{1 + \left(\frac{2\delta\gamma}{\kappa q^2}\right)^2} + 1 \right], \qquad (2.22)$$

one finds

$$K_{semi}(q) = \kappa q^4 + \frac{(\delta\gamma)^2}{\kappa} + O\left(\frac{1}{q^4}\right). \qquad (2.23)$$

By Eqs. (2.5) and (2.18),

$$K_{semi}(q) = \kappa q^4 + \frac{B_{sm}}{a} + O\left(\frac{1}{q^4}\right), \qquad (2.24)$$

for $q \gg q_b$. The first leading term in Eq. (2.24) corresponds to the bending elastic energy of a free manifold. This term actually originates from the bending energy of the first, interfacial manifold of the stack, with the height function $h_1(\mathbf{x})$, see Fig. 1. However, this manifold is not really free, as evidenced by the second term in Eqs. (2.23) and (2.24). This term is a constant resembling the standard ''mass'' term in field theories. The origin of this quasimass can be traced from the elastic model in Eq. (2.3) by fixing therein the height $h_2(\mathbf{x})$ of the $n=2$ manifold to a flat immobile configuration. The dispersion relation of the interfacial, $n=1$ manifold would then have the from as in Eq. (2.24) but *without* the $O(1/q^4)$ terms therein. The presence of these terms simply reflects the fact that the $n=2$ manifold is not flat, and, moreover, that it is coupled to the $n=3$ manifold, which itself is coupled to the $n=4$ manifold, and so on. The exact form of the interface dispersion relation in Eq. (2.16) thus reflects the interactions between *all* manifolds in the smectic stack. They ''dress'' the interface manifold $h_1(\mathbf{x})$ in such a way that it is no longer a free one (with dispersion $\simeq \kappa q^4$), but, rather, a dressed one, with the dispersion relation as in Eq. (2.16). To highlight this important feature, in Appendix A we present an alternative discussion of our model in Eqs. (2.15) and (2.16) playing the substantial role in the developments of the following sections.

The interface model in Eqs. (2.15) and (2.16) provides a simple and global approach to handle the interface fluctuation over the entire range of length scales and momentum scales ($q \ll q_b$, $q \gg q_b$, and, also, $q \sim q_b$). This is an essential feature needed for the model's applications detailed in the following sections. Prior to them, we would like to stress some features of our interface model:

(i) The model has been derived by means of the harmonic approximation Eq. (2.3) to the effective anharmonic stack model Eq. (2.1). The interface model in Eq. (2.15) is thus a harmonic model, quadratic in the interface shape $h_1(\mathbf{x})$. Anharmonic terms may have been included in Eq. (2.15) along similar lines, by considering the full anharmonic stack model. In a practical application of the harmonic interface model, such anharmonic effects can be ignored if one can (self-consistently) confirm that the local smectic strains are small, $e_n = [h_{n+1}(\mathbf{x}) - h_n(\mathbf{x}) - a]/a = [u_{n+1}(\mathbf{x}) - u_n(\mathbf{x})]/a \ll 1$ for all manifolds within the semi-infinite stack. On the other hand, in our applications to the sterically stabilized phases (see Sec. IV), one typically has $e_n = O(1)$ (for the manifolds neighboring the small stack, see Secs. III and IV). Still, even for this application, the harmonic interface model, Eq. (2.15), provides a reasonable approximation to the exact anharmonic interface model, as evidenced by the results discussed in Sec. IV.

(ii) The effective anharmonic model, Eq. (2.1), as well as a more microscopic model discussed in Sec. III, ignore bending energy anharmonicities yielding the softening of the manifold rigidity κ, for $d=2$ (fluid membrane) and $d=1$ (semiflexible polymers), due to crumpling effects [21]. These effects may be significant in the sterically stabilized phases [11]. However, even in these phases, the softening of the bending rigidity κ can be ignored if $a \ll \xi_p$, the manifold persistence length [11]. We will confine our discussion to the limit $a/\xi_p \ll 1$, and ignore the crumpling effects. Most of the related theoretical studies have assumed the limit $a/\xi_p \ll 1$, in part, because it is frequently experimentally realized (e.g., in very recent studies Refs. [3–5]). These effects are qualitatively substantial only in sterically stabilized phases with $a \sim \xi_p$. Such a smectic is close to the phase transition line to isotropic liquid phase [8,25]. We will, however, confine our discussions to the region $a \ll \xi_p$, away from this transition line.

(iii) Finally, the effective stack model, Eq. (2.1), as well as a more microscopic stack model discussed in Sec. III, both break rotational invariance by assuming that interactions depend on the ''vertical distance'' $h_{n+1}(\mathbf{x})-h_n(\mathbf{x})$ between manifolds. The resulting harmonic model (2.3) is still the standard Landau-Peierls harmonic smectic model [14], as one can see by assuming in Eq. (2.3) the usual continuum limit, $z=na$ and $u_n(\mathbf{x})=u(z,\mathbf{x})$ therein. However, the vertical distance approximation suppresses the anharmonic terms that are, in the full nonlinear smectic model, responsible for the anomalous elasticity effects present in 3D smectic liquid crystals [16], as well as in 2D smectic liquid crystals [2]. In this paper, we ignore these effects, in part because they are usually quantitatively weak, for example, in the recently studied experimental systems [3,4], as discussed in more detail in Refs. [7,8,23]. Besides, as already noted in Ref. [8], the anomalous elasticity effects are pressumably exactly canceled in the interfacial model for 2D smectic liquid crystals, which are in the focus of our investigation (see Sec. IV): Anomalous elasticity produces a substantial length scale dependence (renormalization) of the smectic elastic constants K_{sm} and B_{sm} at long length scales. It may thus qualitatively modify only the small q interfacial behavior in Eq. (2.21), with $\delta\gamma=\sqrt{K_{sm}B_{sm}}$ therein replaced by the momentum dependent tension $\delta\gamma(q)=\sqrt{K_{sm}(q)B_{sm}(q)}$, with the momentum dependent smectic elastic constants $K_{sm}(q)$ and $B_{sm}(q)$. However, by Ref. [2], for 2D smectic liquid crystals one has exactly $K_{sm}\sim 1/q^{1/2}$ and $B_{sm}\sim q^{1/2}$ at small q, as found by an exact mapping of 2D smectic liquid crystals onto the Kardar-Parisi-Zhang model. Thus, accidentally, the product $K_{sm}(q)B_{sm}(q)$, entering the tension $\delta\gamma(q)$, is *not* length scale dependent in 2D smectic liquid crystals, indicating the cancellation of the anomalous elasticity effects in the exact interfacial model for these systems.

III. SMALL SUBSYSTEMS OF INFINITE SMECTIC STACKS

Here, we use our interface Hamiltonian of Sec. II to develop an efficient approach to the statistical mechanics of infinite stacks of flexible manifolds, such as two-dimensional smectic phases of long semiflexible polymers and three-dimensional lamellar fluid membrane phases. Within our approach, the practically interesting thermodynamic limit, with infinite number of manifolds, is reduced to considering a small stack, with just a few interacting manifolds, representing a subsystem of an infinite smectic liquid crystal. This dramatic reduction in the number of degrees of freedom is achieved by treating the first (the last) manifold of the small stack as an interface with the semi-infinite smectic medium below (above) the small stack, as detailed in the following.

The objects of our discussion here are *microscopic* smectic stack Hamiltonians in the constant pressure ensemble [8,23] of the form

$$H_{mic}(\{h_n\})=\int d^d\mathbf{x}\Bigg[\sum_{n=-\infty}^{\infty}\{P[h_{n+1}(\mathbf{x})-h_n(\mathbf{x})] + V(h_{n+1}(\mathbf{x})-h_n(\mathbf{x}))\} + \sum_{n=-\infty}^{\infty}\frac{\kappa}{2}\left(\frac{\partial^2 h_n(\mathbf{x})}{\partial \mathbf{x}^2}\right)^2\Bigg]. \tag{3.1}$$

Here, in contrast to the effective stack Hamiltonian (2.1), $V(h_{n+1}(\mathbf{x})-h_n(\mathbf{x}))$ in Eq. (3.1) represents the actual (microscopic) interaction potential between fluctuating manifolds. We assume here only the nearest neighbors interaction in the stack. Further neighbors interaction can be included in the theory, but at the expense of the simplicity and clarity needed in this discussion. We note, however, that for the interesting case of sterically stabilized smectic phases, with purely hard-core repulsion, one has (by definition) only the nearest neighbors interaction. To proceed, we split the manifolds in Eq. (3.1) into three groups: (i) the ''small stack'' comprised of M manifolds, with $n=1,2,3,\ldots,M$; (ii) the upper smectic medium, comprised of the manifolds with $n=M+1,M+2,\ldots,\infty$; and (iii) the lower smectic medium, comprised of remaining manifolds with $n=0,-1,-2,\ldots,\infty$. This partition of the stack is conceptualized in Fig. 2. We perform a corresponding division also in Hamiltonian (3.1), by writing it as

$$H_{mic}=H_{small}(h_1,h_2,\ldots,h_M)+H_{upper}(h_M,h_{M+1},\ldots) + H_{lower}(h_1,h_0,h_{-1},h_{-2},\ldots), \tag{3.2}$$

with $H_{small}(h_1,h_2,\ldots,h_M)$ of the form as in Eq. (3.1), but with the first sum running from $n=1$ to $n=M-1$, and the second sum running from $n=2$ to $n=M-1$. Likewise, $H_{upper}(h_M,h_{M+1},\ldots)$ also has the form as in Eq. (3.1), but with both sums running from $n=M$ to $n=+\infty$. Finally, $H_{lower}(h_1,h_0,h_{-1},h_{-2},\ldots)$ also has the form as Eq. (3.1), but with first sum running from $n=-\infty$ to $n=0$, and the second sum running from $n=-\infty$ to $n=1$. The virtue of the partition in Eq. (3.2) is seen by considering the infinite stack partition function

$$Z=\prod_{n=-\infty}^{\infty}\int Dh_n\, e^{-H_{mic}(\{h_n\})/k_BT}, \tag{3.3}$$

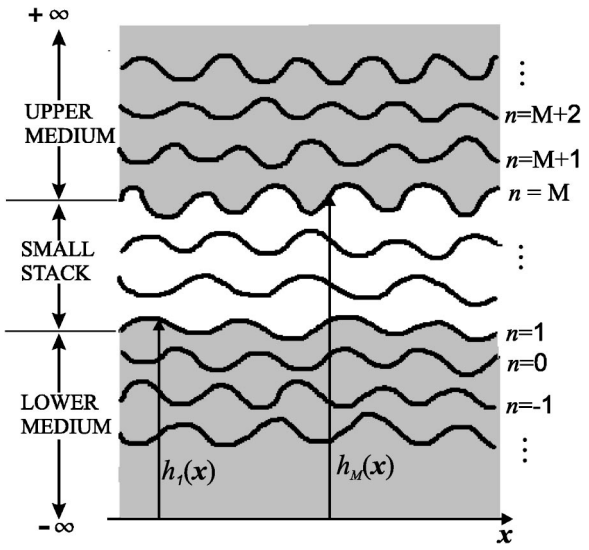

FIG. 2. The partition of an infinite smectic stack of manifolds with the height functions $h_n(\mathbf{x})$ into the "small stack" ($n=1,2,\ldots,M$), the "upper medium" ($n=M+1,M+2,\ldots$), and the "lower medium" ($n=0,-1,-2,\ldots$). Here, $h_1(\mathbf{x})$ and $h_M(\mathbf{x})$ are the interfacial manifolds.

which is easily shown to be *exactly* equal to

$$Z=\prod_{n=1}^{M}\int Dh_n\, e^{-H_{small}^{(eff)}(h_1,h_2,\ldots,h_M)/k_BT}. \tag{3.4}$$

Here, $H_{small}^{(eff)}$ is the *effective* Hamiltonian of the small stack of the form

$$H_{small}^{(eff)}(h_1,h_2,\ldots,h_M)=H_{small}(h_1,h_2,\ldots,h_M)+H_{int}^{(low)}(h_1)+H_{int}^{(up)}(h_M). \tag{3.5}$$

In Eq. (3.5),

$$H_{int}^{(up)}(h_M)=-k_BT\ln\left\{\prod_{n=M+1}^{\infty}\int Dh_n\, e^{-H_{upper}(h_M,h_{M+1},\ldots)/k_BT}\right\} \tag{3.6}$$

is the effective Hamiltonian for the interfacial manifold $h_M(\mathbf{x})$, whereas

$$H_{int}^{(low)}(h_1)=-k_BT\ln\left\{\prod_{n=-\infty}^{0}\int Dh_n\, e^{-H_{lower}(h_1,h_0,h_{-1},\ldots)/k_BT}\right\} \tag{3.7}$$

is the effective Hamiltonian for the interfacial manifold $h_1(\mathbf{x})$. It is easy to show that the *forms* of the two interfacial Hamiltonians defined by Eqs. (3.6) and (3.7) are entirely the same. More precisely, $H_{int}^{(low)}(h)=H_{int}^{(up)}(-h)$.

By the above construction, any infinite smectic average involving the degrees of freedom of the small stack can be obtained *exactly* by using the effective Hamiltonian of the small stack $H_{small}^{(eff)}$ defined by Eq. (3.5). In particular, the interesting average

$$a(P)=\langle h_{n+1}(\mathbf{x})-h_n(\mathbf{x})\rangle_P \tag{3.8}$$

giving the equilibrium value of the smectic phase period a as a function of the isotropic osmotic pressure P (i.e., the smectic equation of state) can be obtained exactly either by using the infinite smectic stack Hamiltonian (3.1), or by using the effective small stack Hamitonian, Eq. (3.5), with h_n and h_{n+1} being the members of the small stack. In fact, remarkably, to obtain the infinite smectic equation of state in Eq. (3.8), it suffices to consider the effective Hamiltonian of the small stack with just $M=2$ manifolds $h_1(\mathbf{x})$ and $h_2(\mathbf{x})$, and use it to calculate the average

$$a(P)=\langle h_2(\mathbf{x})-h_1(\mathbf{x})\rangle_{P,M=2}.$$

By the virtue of our definition of $H_{small}^{(eff)}$, this small stack average is exactly equal to that obtained by considering the infinite smectic stack, or by considering the small stack with just M manifolds (any M) and using its effective Hamiltonian to calculate *any* of the $M-1$ averages

$$a(P)=\langle h_{n+1}(\mathbf{x})-h_n(\mathbf{x})\rangle_{P,M},\quad n=1,2,\ldots,M-1.$$

They are all equal to each other, and thus equal to the average

$$a(P)=\left\langle\frac{h_M(\mathbf{x})-h_1(\mathbf{x})}{M-1}\right\rangle_{P,M}. \tag{3.9}$$

Thus, by using $H_{small}^{(eff)}$, the original difficult problem of the infinite stack is reduced to that of the small stack with just a few manifolds ($M=2,3$, or so).

Technical feature of using the effective small stack Hamiltonian, Eq. (3.5), is that it requires the exact form of the interfacial Hamiltonian in Eq. (3.6) [or in Eq. (3.7)]. H_{int} can be found, in principle, by doing the reduced partition function in Eq. (3.6), for a fixed shape of the interfacial manifold $h_M(\mathbf{x})$. Equivalently, in the spirit of Sec. II, this problem can be solved by using the appropriate effective Hamiltonian $H_{upper}^{(eff)}(h_M,h_{M+1},\ldots)$ of the upper medium and minimizing it over $h_{M+1}(\mathbf{x})$, $h_{M+2}(\mathbf{x})$, ..., for a fixed $h_M(\mathbf{x})$. In practice, none of these procedures can be implemented exactly, and one must resort to sound approximations to H_{int}. The harmonic interfacial Hamiltonian derived in Sec. II is the most natural first candidate for this purpose. It has the desirable property (necessary for the present purpose) that it can be applied to interfacial fluctuations of all length scales, see Sec. II. Thus, we will approximate the exact H_{int} with interfacial Hamiltonian defined in Eqs. (2.15) and (2.16). Consequently, the exact small stack effective Hamiltonian, Eq. (3.5), is approximated by

$$
\begin{aligned}
H_{small}^{(eff)}(h_1,h_2,\ldots,h_M) &= \frac{1}{2}\int \frac{d^dq}{(2\pi)^d} K_{semi}(q)|\tilde{h}_1(\mathbf{q})|^2 \\
&+ \frac{1}{2}\int \frac{d^dq}{(2\pi)^d} K_{semi}(q)|\tilde{h}_M(\mathbf{q})|^2 \\
&+ \sum_{n=2}^{M-1} \int \frac{d^dq}{(2\pi)^d}\frac{\kappa}{2}q^4|\tilde{h}_n(\mathbf{q})|^2 \\
&+ \sum_{n=1}^{M-1} \int d^dx\{V(h_{n+1}(\mathbf{x})-h_n(\mathbf{x})) \\
&+ P[h_{n+1}(\mathbf{x})-h_n(\mathbf{x})]\} \qquad (3.10)
\end{aligned}
$$

with $K_{semi}(q)$ defined in Eq. (2.16). It is important to stress that this approximation can be controlled. This can be done by calculating the practically significant average in Eq. (3.9) by using the approximative small stack Hamiltonian in Eq. (3.10). Let us denote this average as

$$
a=\left\langle \frac{h_M(\mathbf{x})-h_1(\mathbf{x})}{M-1}\right\rangle_M \equiv f_M\left(P,\frac{dP}{da}\right). \qquad (3.11)
$$

Recall that, for the *exact* $H_{small}^{(eff)}$, the average in Eq. (3.11) would be M independent. With a good *approximative* $H_{small}^{(eff)}$, however, one may expect that the average in Eq. (3.11) only weakly depends on M, and that the thermodynamic limit is quickly approached with increasing M. Our approximative $H_{small}^{(eff)}$ in Eq. (3.10) indeed provides such quick convergence to the *exact* thermodynamic limit behavior even in the case of highly anharmonic sterically stabilized phases, as documented in Sec. IV.

Note that the average in Eq. (3.11) depends not only on P, but also on (dP/da) [as emphasized in Eq. (3.11)]. This is because this derivative actually enters the dispersion relation $K_{semi}(q)$ in the effective small stack Hamitonian (3.10) [see Eqs. (2.16) and (2.18)]. Next, note that with a known form of the function f_M in Eq. (3.11), this equation represents the first-order ordinary differential equation for the function $P(a)$. Solving it eventually yields the desired equation of state $P(a)$. In the following section, we illustrate this procedure by considering the interesting example of sterically stabilized smectic stacks of d-dimensional manifolds.

IV. STERICALLY STABILIZED SMECTIC LIQUID CRYSTALS

In this section, the approach of Sec. III is illustrated by considering in detail the difficult statistical mechanics problem of sterically stabilized smectics of flexible manifolds with hard-core repulsion [9–11,17,21–23]. We will show here that the exact thermodynamic limit equation of state and universal constants characterizing entropic elasticity in these phases can be obtained with a high accuracy already from numerical simulations involving small stacks with just a few manifolds. In these smectic systems, the intermanifold potential is the hard-core repulsion potential, of the form

$$
V_{hc}(r)=\begin{cases} 0, & r>0 \\ \infty, & r<0, \end{cases} \qquad (4.1)
$$

with $r=h_{n+1}(\mathbf{x})-h_n(\mathbf{x})$. To proceed, it will be convenient to transform the reduced effective Hamiltonian of the small stack, Eq. (3.10), $H_{small}^{(eff)}/k_BT$ into a dimensionless form. In fact, for $d<4$, the stack model has a finite continuum limit $\Delta x\to 0$ [23], and can be thus freely rescaled as

$$
\mathbf{x}=L_x\mathbf{x}', \quad h_n(\mathbf{x})=L_h h_n'(\mathbf{x}'), \qquad (4.2)
$$

with arbitrary rescaling constants (length units) L_x and L_h. [In terms of momentum variables in Eq. (3.10), this corresponds to $\mathbf{q}=(L_x)^{-1}\mathbf{q}'$ and $\tilde{h}_n(\mathbf{q})=L_h(L_x)^{-d}\tilde{h}_n'(\mathbf{q}')$.] Note that the hard-core potential in Eq. (4.1) is actually invariant under any rescaling, as $V_{hc}(h_{n+1}(\mathbf{x})-h_n(\mathbf{x}))=V_{hc}(h_{n+1}'(\mathbf{x}')-h_n'(\mathbf{x}'))$. Under this rescaling, Eq. (3.11) transforms simply as

$$
a=\left\langle \frac{h_M(\mathbf{x})-h_1(\mathbf{x})}{M-1}\right\rangle = L_h\left\langle \frac{h_M'(\mathbf{x}')-h_1'(\mathbf{x}')}{M-1}\right\rangle. \qquad (4.3)
$$

A convenient choice for the length unit L_x is to identify it with the healing length L_b, see Eq. (2.19) and (2.20). This is the unique length scale present in the interfacial dispersion relation $K_{semi}(q)$ that enters the small stack Hamiltonian (3.10), see Sec. II and Eq. (4.11) below. Thus, we set

$$
L_x=L_b=\left(\frac{\kappa}{-\dfrac{dP}{da}}\right)^{1/4}. \qquad (4.4)
$$

Next, some thought suggests that the convenient choice for the length unit L_h is

$$
L_h=a\Omega\Pi, \qquad (4.5)
$$

where Ω and Π are dimensionless quantities defined by

$$
\Omega=\frac{P(a)}{-a\dfrac{dP(a)}{da}}=-\frac{1}{\dfrac{d\ln P(a)}{d\ln a}} \qquad (4.6)
$$

and

$$
\Pi=\sqrt{\frac{P^{1-d/4}a^{1+d/4}\kappa^{d/4}}{k_BT}}\Omega^{1+d/4}. \qquad (4.7)
$$

With the above choice of L_h, Eq. (4.3) yields the equation

$$
\frac{1}{\Omega}=\frac{f_{M,d}(\Pi)}{\Pi}. \qquad (4.8)
$$

Here,

$$
f_{M,d}(\Pi)=\left\langle \frac{h_M'(\mathbf{x}')-h_1'(\mathbf{x}')}{M-1}\right\rangle_{\Pi,M}, \qquad (4.9)
$$

where the equilibrium average is done with respect to the rescaled reduced small stack effective Hamiltonian

$$\begin{aligned}\bar{H}_{\Pi}(\{h'\}) &= \frac{H_{small}^{(eff)}}{k_B T} \\ &= \frac{1}{2}\int \frac{d^d q'}{(2\pi)^d} K'_{semi}(q')|\tilde{h}'_1(\mathbf{q}')|^2 \\ &\quad + \frac{1}{2}\int \frac{d^d q'}{(2\pi)^d} K'_{semi}(q')|\tilde{h}'_M(\mathbf{q}')|^2 \\ &\quad + \frac{1}{2}\sum_{n=2}^{M-1}\int \frac{d^d q'}{(2\pi)^d}(q')^4|\tilde{h}'_n(\mathbf{q}')|^2 \\ &\quad + \sum_{n=1}^{M-1}\int d^d x'\{V_{hc}(h'_{n+1}(\mathbf{x}')-h'_n(\mathbf{x}')) \\ &\quad + \Pi[h'_{n+1}(\mathbf{x}')-h'_n(\mathbf{x}')]\} \end{aligned} \tag{4.10}$$

with

$$K'_{semi}(q') = \sqrt{(q'^2)^2 + \left(\frac{q'^4}{2}\right)^2} + \frac{q'^4}{2}. \tag{4.11}$$

Notably, the only continuous parameter entering the Hamiltonian in Eq. (4.10) [and, thus, the average in Eq. (4.9)] is the dimensionless pressure Π. The universal shape of the function $f_{M,d}(\Pi)$ can be obtained by calculating the equilibrium average in Eq. (4.9), e.g., by Monte Carlo (MC) simulations, as done in the following. For that purpose, we used the translational invariance of the system (along the **x** directions), implying

$$f_{M,d}(\Pi) = \langle \rho \rangle \tag{4.12}$$

with

$$\rho = \frac{\int d^d x'[h'_M(\mathbf{x}')-h'_1(\mathbf{x}')]}{A_B(M-1)}. \tag{4.13}$$

Here, $A_B = \int d^d x'$ is the stack base area. Eqs. (4.12) and (4.13) provide an efficient way of obtaining accurate form of $f_{M,d}(\Pi)$ from MC simulations, as discussed in Appendix B. Once the form of $f_{M,d}(\Pi)$ is known, one may proceed to calculate the equation of state $P(a)$. This can be done by solving the first-order differential equation for $P(a)$ that is obtained by combining Eqs. (4.6) through (4.8) [see, also, the end of Sec. III]. The equation of state corresponds to the physical solution of this equation, with $P(a)\to 0$ as $a\to\infty$. This solution can be easily found by noting that Eqs. (4.6) through (4.8) are consistent with $P(a)$ decaying as a power law of a. For this solution, Ω in Eq. (4.6) is simply a constant, and thus, by Eq. (4.8), Π is a constant. Thus, by Eq. (4.7), we obtain the smectic equation of state in the form

$$P(a) = \bar{\alpha}_M(d)\frac{(k_B T)^{4/(4-d)}}{\kappa^{d/(4-d)} a^{(4+d)/(4-d)}} \tag{4.14}$$

with the universal constant

$$\bar{\alpha}_M(d) = \frac{\Pi^{8/(4-d)}}{\Omega^{(4+d)/(4-d)}}. \tag{4.15}$$

Here, by Eqs. (4.14) and (4.6), one obtains

$$\Omega = \frac{4-d}{4+d} \tag{4.16}$$

yielding further, by Eq. (4.8),

$$\frac{4+d}{4-d} = \frac{f_{M,d}(\Pi)}{\Pi}. \tag{4.17}$$

Thus, by Eqs. (4.17) and (4.15),

$$\bar{\alpha}_M(d) = \left(\frac{4+d}{4-d}\right)^{(4+d)/(4-d)} \Pi^{8/(4-d)}, \tag{4.18}$$

where Π is a universal constant to be found by solving Eq. (4.17) with a known form of the function $f_{M,d}(\Pi)$.

To summarize the above algorithm: The universal constant $\bar{\alpha}_M(d)$ in the smectic equation of state (4.14) can be found by Eq. (4.18), with Π therein found by solving Eq. (4.17), with the function $f_{M,d}(\Pi)$ therein found by doing the average in Eq. (4.12) with respect to the Hamiltonian (4.10). This procedure yields the universal constant $\bar{\alpha}_M(d)$ that depends not only on the manifold dimension d, but also on the number of manifolds in the small stack M. This M dependence reflects the approximative nature of the interface Hamiltonian (for the manifolds h_1 and h_M) that has been used in the approximative small stack effective Hamiltonian Eq. (3.10): As discussed in Sec. III, with the exact interface Hamiltonian, there would be *no* M dependence in the equation of state, that is, $\bar{\alpha}_M(d)$ would be M independent. Thus, with a *good* approximative interfacial Hamiltonian, $\bar{\alpha}_M(d)$ should only weakly depend on M. In particular, the constant $\bar{\alpha}_2(d)$ should be approximately equal to the constant $\bar{\alpha}_\infty(d)$, which itself *afortiori* coincides with the *exact* value of this constant in the infinite smectic stack equation of state (as, for $M\to\infty$, the thermodynamic limit is approached anyway.) If $\bar{\alpha}_2(d)\approx\bar{\alpha}_\infty(d)$, the exact thermodynamic limit (bulk) properties, such as the system's equation of state, are rapidly asymtotically approached by using small stacks with just a few manifolds ($M=2,3$, or so).

To examplify these features, here we consider 2D smectic phases of long semiflexible polymers ($d=1$ case). In fact, these low-dimensional sterically stabilized smectic systems exhibit the strongest finite size effects. They thus provide the best test for the approach pursued in this paper. Technical features of the MC simulations used here are similar to those of Ref. [23], with the exception of the crucial interfacial energy terms, i.e., the $K_{semi}(q)$ terms entering the small stack effective Hamiltonian in Eq. (3.10). Their implementation is discussed in Appendix A. The MC simulations are used to obtain the universal function $f_{M,d}(\Pi)$ in Eq. (4.9), for stacks with $M=2$ through six semiflexible polymers ($d=1$). The accurate shape of this function is needed only for

TABLE I. Universal constants $\bar{\alpha}_M(1)$ characterizing the entropic repulsion pressure in 2D small stacks of M semiflexible polymers [governed by the effective Hamiltonian (3.10)]. The finite M data are well fitted by the extrapolation formula $\bar{\alpha}_M(1)=\bar{\alpha}_\infty(1)+\bar{C}_{(1)}M^{-1}+\bar{C}_{(3/2)}M^{-3/2}$ (see Ref. [23], with $\bar{\alpha}_\infty(1)=0.433$, $\bar{C}_{(1)}=0.060$, and $\bar{C}_{(3/2)}=-0.010$, as indicated in the table.

M	2	3	4	5	6	∞
$\bar{\alpha}_M(1)$	0.456 ± 0.002	0.451 ± 0.002	0.447 ± 0.002	0.444 ± 0.003	0.442 ± 0.003	0.433[a]

[a]Obtained by the extrapolation formula.

the Π's in the vicinity of the solution to Eq. (4.17) that we need to obtain the universal constants $\bar{\alpha}_M(d)$ by Eq. (4.18). In Appendix B, we describe the strategy used to obtain the needed form of $f_{M,d}(\Pi)$. Our results for the constants $\bar{\alpha}_M(d=1)$ are listed in Table I. The Table also gives the estimated value of $\bar{\alpha}_\infty(d=1)$ entering the (thermodynamic limit) equation of state for the sterically stabilized 2D smectic stacks of semiflexible polymers, which is, by Eq. (4.14), with $d=1$,

$$P(a)=\bar{\alpha}_\infty(1)\frac{(k_BT)^{4/3}}{\kappa^{1/3}a^{5/3}} \tag{4.19}$$

with $\bar{\alpha}_\infty(1)\cong 0.433$, as discussed hereafter. From the table, we see that $\bar{\alpha}_2(1)$ is only some 4% bigger than $\bar{\alpha}_\infty(1)$. Thus, by using our simple interfacial model of Sec. II incorporated into the small stack effective Hamiltonian (3.10), the thermodynamic limit (bulk) properties can be very accurately investigated by using small smectic stacks with just a few manifolds. Figure 3 gives the constant $\bar{\alpha}_M(1)$ versus M (open circles). By discussions similar to those of Ref. [23], here one has the asymptotic expansion

$$\bar{\alpha}_M(1)=\bar{\alpha}_\infty(1)+\frac{\bar{C}_{(1)}}{M}+\frac{\bar{C}_{(3/2)}}{M^{3/2}}+\frac{\bar{C}_{(2)}}{M^2}+\frac{\bar{C}_{(5/2)}}{M^{5/2}}+\cdots \tag{4.20}$$

with C constants dependent on boundary conditions (character of interfacial manifolds). Our data in Table I are well fit by Eq. (4.20) with $\bar{\alpha}_\infty(1)=0.433$, $\bar{C}_{(1)}=0.060$, and $\bar{C}_{(3/2)}=-0.010$ and other constants zero, see the inset Fig. 3. In Fig. 3, we also present, for comparision, the constants $\alpha_M(1)$ entering the equation of state in the recently studied constant pressure ensemble of M manifolds [23]. In this ensemble, the elastic energy of interfacial manifolds is just their bending energy, in contrast to more complex elastic energy of the interfacial manifolds used here in the small stack effective Hamiltonian, see Eqs. (3.10) and (2.16). Such a constant pressure ensemble thus represents an approximation to our approach here, with $K_{semi}(q)$ in Eq. (2.16) approximated by κq^4. For this ensemble, the equation of state is again as in Eq. (4.14), however, with different prefactors, $\alpha_M(1)$ obtained in Ref. [23] and given here in Fig. 3 for comparision (full squares). Notably from the figure, $\alpha_M(1)>\bar{\alpha}_M(1)>\bar{\alpha}_\infty(1)$, and both sequences $\alpha_M(1)$ and $\bar{\alpha}_M(1)$ approach $\bar{\alpha}_\infty(1)$ as $M\to\infty$. Still, the sequence $\bar{\alpha}_M(1)$ has a significantly better asymptotic approach, see the inset of Fig. 3 and Fig. 3 caption. Note that, for example, the constant $\bar{\alpha}_2(1)$, for the small stack of just two manifolds, has nearly the same value as $\alpha_6(1)$, for the constant pressure ensemble of six manifolds!

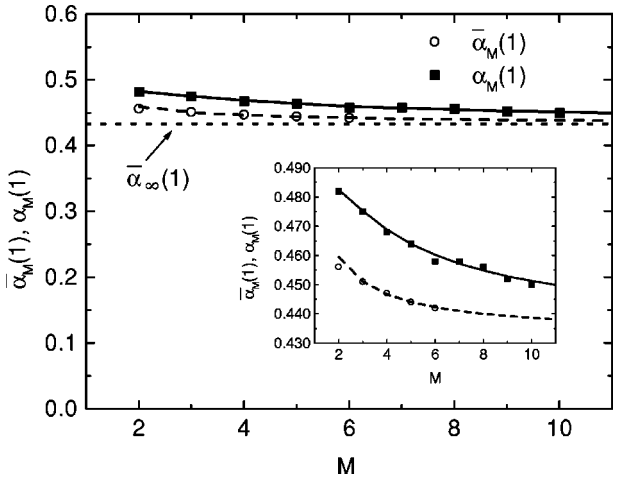

FIG. 3. Universal constants $\bar{\alpha}_M(1)$ for the small stack equation of the state, Eq. (4.14), versus the number of manifolds M (open circles). The dashed line is the fit to data in Table I, of the form $\bar{\alpha}_\infty(1)+\bar{C}_{(1)}M^{-1}+\bar{C}_{(3/2)}M^{-3/2}$, with $\bar{\alpha}_\infty(1)=0.433$, $\bar{C}_{(1)}=0.060$, and $\bar{C}_{(3/2)}=-0.010$. For comparision, we present also the universal constants $\alpha_M(1)$ for stacks of M manifolds in the constant pressure ensemble. See Ref. [23] (filled square). The solid line is the fit $\alpha_\infty(1)+C_{(1)}M^{-1}+C_{(3/2)}M^{-3/2}$ with $\alpha_\infty(1)=0.433$, $C_{(1)}=0.250$, and $C_{(3/2)}=-0.213$.

V. SUMMARY AND OUTLOOK

In this paper, we have elucidated the classical problem of the elastic free energy of semi-infinite smectic-*A* liquid crystal that fills a semispace above a boundary smectic layer (interface) of a given shape. For the free energy of this interface, we have obtained an effective interface Hamiltonian that takes into account discreteness due to the layered character of smectic-*A* phases. The interface model is thus applicable to both short and long wavelength fluctuations of the interface shape. Further, we have used our Hamiltonian to develop an efficient approach to the statistical thermodynamics of stacks of N flexible manifolds, such as two-dimensional smectic phases of long semiflexible polymers and three-dimensional lamellar fluid membrane phases.

Within our approach, the practically interesting thermodynamic limit $N\to\infty$ is reduced to considering a small stack with a few interacting manifolds representing a subsystem of the infinite smectic. This has been achieved by treating the first (the last) manifold of the small stack as an interface with the semi-infinite smectic medium below (above) the manifold. We have documented our approach by considering in detail two-dimensional sterically stabilized smectic liquid crystals of long semiflexible polymers with hard-core repulsion. The exact equation of state and universal constants characterizing entropic elasticity in these phases in the thermodynamic limit are obtained, with a high accuracy, already from numerical simulation of small smectic subsystems involving just a few semiflexible polymers.

Finally, we anticipate some future application of the approach introduced here. By using it, one can systematically address the long standing problem of the quantitatively strong entropic effects on the equation of state of the bound stacks of fluid membranes, that are stable even at zero osmotic pressure [26]. Likewise, the recently experimentally observed unbinding transition of such stacks [27] can also be addressed along the line pursued in the present paper. All these theoretically hard, but experimentally interesting problems, deserve systematic studies to be pursued in future subsequent works.

ACKNOWLEDGMENTS

We thank Joachim Raedler, Tim Salditt, and Cyrus Safinya for various discussions on semiflexible polymer phases. L.G. acknowledges support through Grant No. A/02/15054 of the Deutscher Akademischer Austauschdienst (DAAD).

APPENDIX A

Here we present an alternative derivation of the smectic interface model of Sec. II. Deeply related to this discussion is our method to implement, in MC simulations of Sec. IV, the interfacial terms of the small stack of effective Hamiltonian (see Sec. III). This method is also discussed here. For these purposes, we consider the elastic model, Eq. (2.22), in a slightly more general form

$$H_{el}=\int_q\left[\sum_{n=1}^{N}\frac{1}{2}K_n(q)|\tilde{u}_n(\mathbf{q})|^2+\sum_{n=1}^{N-1}\frac{B}{2}|\tilde{u}_{n+1}(\mathbf{q})-\tilde{u}_n(\mathbf{q})|^2\right] \tag{A1}$$

with $\int_q=\int d^dq/(2\pi)^d$. For the smectic stack, $B=V''_{eff}(a)=-\partial P(a)/\partial a=B_{sm}(a)/a$ and $K_n(q)=\kappa q^4$ for all values of n. Still, for the future convenience, we allow here $K_n(q)$ having different forms for different manifolds in the stack. The manifolds u_1 and u_N in Eq. (A1) are the ''interfacial'' manifolds, at the bottom and the top of the stack. For convenience, we discuss the construction of the interface Hamiltonian for u_N, rather than u_1, as done in Sec. II [obviously, if $K_n(q)$ have the same form for all n's, the forms of interfacial Hamiltonians for u_1 and u_N are the same]. As in Sec. II, we want to minimize H_{el} in Eq. (A1) for a fixed shape of the interface $u_N(\mathbf{x})$. Here we will do this in *steps*: in the first step, we minimize over u_1, in the second step we minimize over u_2, etc. By the form of H_{el} in Eq. (A1), it is not hard to show that after m steps, the minimized elastic energy has the form

$$(H_{el})_{m\ steps}=\int_q\left[\frac{1}{2}K^{(ren)}_{m+1}(q)|\tilde{u}_{m+1}(\mathbf{q})|^2+\sum_{n=m+2}^{N}\frac{1}{2}K_n(q)|\tilde{u}_n(\mathbf{q})|^2+\sum_{n=m+1}^{N-1}\frac{B}{2}|\tilde{u}_{n+1}(\mathbf{q})-\tilde{u}_n(\mathbf{q})|^2\right] \tag{A2}$$

that depends only on the manifolds $(u_{m+1},u_{m+2},\ldots,u_N)$, as the manifolds $(u_1,u_2,\ldots,u_m)$ are integrated out of the partition function of the harmonic Hamiltonian, Eq. (A1). By comparing Eq. (A1) with Eq. (A2), we see that the effect of the m-step minimization is to replace the bare dispersion relation of the $(m+1)$-st manifold $K_{m+1}(q)$ with a dressed (''renormalized'') dispersion relation $K^{(ren)}_{m+1}(q)$. By using the above step-by-step minimization strategy, it can be easily shown that the renormalized dispersion relations satisfy the recursion relation

$$K^{(ren)}_{m+1}(q)=K_{m+1}(q)+B-\frac{B^2}{B+K^{(ren)}_m(q)}. \tag{A3}$$

For the smectic stack, $K_m(q)=\kappa q^4$ for any m. Thus, by Eq. (A3),

$$K^{(ren)}_{m+1}(q)=\kappa q^4+B-\frac{B^2}{B+K^{(ren)}_m(q)}. \tag{A4}$$

After $m=N-1$ steps, all the manifolds are integrated out, except of the interfacial manifold u_N, for which Eq. (A2) reduces to the desired interfacial Hamiltonian

$$H_{int}(u_N)=(H_{el})_{(N-1)-steps}=\int_q\frac{1}{2}K^{(ren)}_N(q)|\tilde{u}_N(\mathbf{q})|^2. \tag{A5}$$

Here, $K^{(ren)}_N(q)$ is the desired interface dispersion relation. It can be obtained simply by applying $(N-1)$ times the recursion relation in Eq. (A4) , with $m=1,2,\ldots,N-1$, and the ''initial condition'' $K^{(ren)}_{m=1}(q)\equiv\kappa q^4$. In the practically interesting limit $N\to\infty$ [semi-infinite smectic liquid crystal], the interface dispersion relation in Eq. (A5), $K^{(ren)}_N(q)\to K_{semi}(q)$, where $K_{semi}(q)$ is the stable *fixed point* of the recursive mapping in Eq. (A4), i.e.,

$$K_{semi}(q)=\kappa q^4+B-\frac{B^2}{B+K_{semi}(q)}. \tag{A6}$$

Solving Eq. (A6) yields, for the stable fixed point,

$$K_{semi}(q)=\sqrt{\kappa B(q^2)^2+\left(\frac{\kappa q^4}{2}\right)^2}+\frac{\kappa q^4}{2} \tag{A7}$$

in accord with the result of Sec. II [see Eqs. (2.16) and (2.18), with $B=-\partial P/\partial a$ therein].

The above alternative derivation of $K_{semi}(q)$ provides a useful idea discussed in the following, on how to implement the interfacial Hamiltonian $H_{int}(u)$ into the numerical calculations such as the Monte Carlo simulations. This implementation is entirely nontrivial, since the form of $K_{semi}(q)$ [which contains *all* powers of q^2 in its expansion] corresponds to essentially *nonlocal* form of H_{int}. This is best seen, for example, by using the form of $K_{semi}(q)$ in Eq. (A6), yielding the interfacial Hamiltonian in the form

$$H_{int}(u_N)=\int d^dx\left[\frac{\kappa}{2}\left(\frac{\partial^2 u_N(\mathbf{x})}{\partial \mathbf{x}^2}\right)^2+\frac{B}{2}[u_N(\mathbf{x})]^2\right] - \int d^dx_1\int d^dx_2 V(\mathbf{x}_1-\mathbf{x}_2)u_N(\mathbf{x}_1)u_N(\mathbf{x}_2) \tag{A8}$$

with the kernel

$$V(\mathbf{x}_1-\mathbf{x}_2)=\int \frac{d^dq}{(2\pi)^d}e^{i\mathbf{q}\cdot(\mathbf{x}_1-\mathbf{x}_2)}\frac{B^2}{B+K_{semi}(q)}. \tag{A9}$$

The second term in Eq. (A8) is a short-range nonlocal interaction causing difficulties in practical implementations of the interfacial Hamiltonian in a Monte Carlo simulation. Though, in principle, one may go ahead and use Eq. (A8), with the nonlocal kernel in Eq. (A9), we decided for a completely different strategy, inspired by the actual physical origin of $K_{semi}(q)$ discussed above. Instead of modeling the interfacial manifold u_N by means of H_{int} in Eq. (A5), as a single entity dressed by the presence of other manifolds in Eq. (A1), one may, for example, easily implement simulations of the entire *local* harmonic Hamiltonian in Eq. (A1). This method would increase the number of the manifolds to be simulated by $N-1$ which is equal to the number of additional ''virtual'' manifolds, with $m=2,3,\ldots,N-1$ in Eq. (A6). Such an approximation would, however, require using a large N [as only for $N\to\infty$ the fixed point, $K_{semi}(q)$, is approached]. Obviously, this approach would not yield a reasonable MC simulation. Still, it suggests the following more subtle idea on how to tackle the problem: Rather than taking $K_n(q)=\kappa q^4$ for all the manifolds, we carefully choose (''tune'') the forms of $K_n(q)$ in such a way that resulting $K_N^{(ren)}(q)$ in Eq. (A5) approximates the $K_{semi}(q)$ with a high precision. In other words, by using specially chosen forms of $K_n(q)$, the resulting $K_N^{(ren)}(q)$ may be made nearly the same as $K_{semi}(q)$. Remarkably, this turns out to be possible, with a high accuracy, just by using a small number of $N-1$ additional virtual manifolds to be included in the simulations inspired by this idea ($N-1=1$ or 2 as detailed below). Crucial for the success of this approach are, as noted above, specially chosen forms of the virtual manifolds' dispersion relations $K_n(q)$ in Eq. (A1). Below, we give two examples for this. We will work with the rescaled model [see Sec. IV, Eqs. (4.2), (4.10), and (4.11)], for which

$$K_{semi}(q)=\sqrt{(q^2)^2+\left(\frac{q^4}{2}\right)^2}+\frac{q^4}{2}$$

[see Eq. (4.11)] corresponding to Eq. (A7) with $\kappa=B=1$. Our first example is

(1) $N-1=1$, i.e., one uses just one additional, virtual manifold u_1, in addition to the real interfacial manifold u_2. We take $K_1(q)$ and $K_2(q)$ in Hamiltonian (A1), to be of the form

$$K_2(q)=q^4,\quad K_1(q)=\sigma q^2+\kappa' q^4. \tag{A10}$$

With this choice, Eq. (A1) reduces to the local Hamiltonian

$$H_{el}=\frac{1}{2}\int d^dx\left[\sigma\left(\frac{\partial u_1(\mathbf{x})}{\partial \mathbf{x}}\right)^2+\kappa'\left(\frac{\partial^2 u_1(\mathbf{x})}{\partial \mathbf{x}^2}\right)^2 +[u_2(\mathbf{x})-u_1(\mathbf{x})]^2+\left(\frac{\partial^2 u_2(\mathbf{x})}{\partial \mathbf{x}^2}\right)^2\right]. \tag{A11}$$

After minimizing Eq. (A11) over u_1, one obtains the interfacial Hamiltonian in Eq. (A5) for u_2, with $K_2^{(ren)}(q)$ therein of the form

$$K_2^{(ren)}(q)=K_2(q)+1-\frac{1}{1+K_1(q)} \tag{A12}$$

as directly obtained by recursion formula (A3) with $B=1$, as in the rescaled model. It is possible to choose the parameter σ and κ' in Eq. (A10) such that $K_2^{(ren)}(q)$ in Eq. (A12) well approximates the actual interface dispersion relation $K_{semi}(q)$, as measured by the relative error $\mathcal{E}$,

$$\mathcal{E}(q)=\frac{K_2^{(ren)}(q)-K_{semi}(q)}{K_{semi}(q)}, \tag{A13}$$

which needs to be uniformly small, for *all* values of q. For example, by choosing, in Eq. (A10),

$$\sigma=0.995,\quad \kappa'=0.57568, \tag{A14}$$

the magnitude of the relative error in Eq. (A13) turns out to be smaller than 0.005 for all values of q. The error can be made even smaller, by using two or more virtual manifolds, as demonstrated in the following example.

(2) $N-1=2$, i.e., one uses two additional, virtual manifolds u_1 and u_2, in addition to the real interfacial manifold u_3. We take $K_1(q)$, $K_2(q)$, and $K_3(q)$ in Hamiltonian (A1), to be of the form

$$K_3(q)=q^4,$$

$$K_2(q)=\sigma'' q^2+\kappa'' q^4,$$

$$K_1(q)=\sigma' q^2+\kappa' q^4. \tag{A15}$$

With this choice, Eq. (A1) reduces to the local Hamiltonian

$$H_{el}=\frac{1}{2}\int d^dx\Bigg[\sigma'\left(\frac{\partial u_1(\mathbf{x})}{\partial \mathbf{x}}\right)^2+\kappa'\left(\frac{\partial^2 u_1(\mathbf{x})}{\partial \mathbf{x}^2}\right)^2 +[u_1(\mathbf{x})-u_2(\mathbf{x})]^2+\sigma''\left(\frac{\partial u_2(\mathbf{x})}{\partial \mathbf{x}}\right)^2+\kappa''\left(\frac{\partial^2 u_2(\mathbf{x})}{\partial \mathbf{x}^2}\right)^2 +[u_2(\mathbf{x})-u_3(\mathbf{x})]^2+\left(\frac{\partial^2 u_3(\mathbf{x})}{\partial \mathbf{x}^2}\right)^2\Bigg]. \tag{A16}$$

After minimizing Eq. (A16) over u_1 and u_2, one finds the interfacial Hamiltonian, Eq. (A5), for u_3, with $K_3^{(ren)}(q)$ therein obtained by recursion formula (A3) applied twice. That is,

$$K_3^{(ren)}(q)=K_3(q)+1-\frac{1}{1+K_2^{(ren)}(q)}, \tag{A17}$$

with $K_2^{(ren)}(q)$ herein given by Eq. (A12). Again, we choose the parameters σ'', κ'', σ', and κ' in Eq. (A15) to obtain a small relative error

$$\mathcal{E}(q)=\frac{K_3^{(ren)}(q)-K_{semi}(q)}{K_{semi}(q)}. \tag{A18}$$

For example, by choosing, in Eq. (A15),

$$\sigma''=0, \quad \kappa''=1.02, \quad \sigma'=0.9995, \quad \kappa'=0.5, \tag{A19}$$

the magnitude of the relative error, Eq. (A18), turns out to be smaller than 4×10^{-4}, for all values of q. Thus, in the scheme with two virtual manifolds, one may approximate $K_{semi}(q)$ with an accuracy some ten times better than that achieved with just one virtual manifold. By further increasing the number of virtual manifolds, the accuracy can be further increased. For our purpose, the accuracy achieved with the above described scheme with two virtual manifolds was more than sufficient.

APPENDIX B

Here we discuss the issues related to calculating the average $f_{M,d}(\Pi)$ in Eq. (4.9). By the translational symmetry, it can be written also as

$$f_{M,d}(\Pi)=\langle\rho\rangle$$

with ρ defined in Eq. (4.13). As discussed in Sec. IV, $f_{M,d}(\Pi)$ is needed with a high accuracy only for the values of Π in the vicinity of the solution to Eq. (4.17) (in order to solve this equation for Π). In practice, this is achieved by first running an MC simulation for several values of Π, yielding an interpolation formula for $f_{M,d}(\rho)$ used to make the first estimate Π of the solution to Eq. (4.17). Next, we performed a single MC simulation at this value of Π and used it to obtain the shape of $f_{M,d}$ in the vicinity of Π. This is accomplished by using the expansion

$$f_{M,d}(\Pi+\Delta\Pi)=f_{M,d}(\Pi)+C_{M,d}(\Pi)\Delta\Pi+O((\Delta\Pi)^2) \tag{B1}$$

with

$$C_{M,d}=\frac{df_{M,d}(\Pi)}{d\Pi}=(M-1)A_B\langle(\rho-\langle\rho\rangle)^2\rangle, \tag{B2}$$

by the fluctuation-dissipation theorem associated with the Hamiltonian in Eq. (4.10). Like $f_{M,d}$ and $C_{M,d}$, the coefficients of all terms in expasion (B1) can be expressed as equilibrium averages involving powers of ρ. All these coefficients can be thus obtained from a *single* MC simulation done at a *single* value of Π. This idea was used to obtain the form of $f_{M,d}(\Pi)$ in the vicinity of the solution to Eq. (4.17), without running numerous MC simulations at various values of Π.

[1] J. Toner and D.R. Nelson, Phys. Rev. B **23**, 316 (1981).

[2] L. Golubović and Z.-G. Wang, Phys. Rev. Lett. **69**, 2535 (1992); Phys. Rev. E **49**, 2567 (1994).

[3] J.O. Raedler, I. Koltover, T. Saldit, and C.R. Safinya, Science **275**, 810 (1997).

[4] T. Salditt, I. Koltover, J.O. Raedler, and C.R. Safinya, Phys. Rev. Lett. **79**, 2582 (1997); Phys. Rev. E **58**, 889 (1998).

[5] F. Artzner, R. Zantl, G. Rapp, and J.O. Raedler, Phys. Rev. Lett. **81**, 5015 (1998); R. Zantl, F. Artzner, G. Rapp, and J.O. Raedler, Europhys. Lett. **45**, 90 (1990).

[6] L. Golubović and M. Golubović, Phys. Rev. Lett. **80**, 4341 (1998); **81**, 5704(E) (1998); C.S. O'Hern and T.C. Lubensky, *ibid.* **81**, 4345 (1998).

[7] L. Golubović, T.C. Lubensky, and C.S. O'Hern, Phys. Rev. E **62**, 1069 (2000).

[8] L. Golubović, Phys. Rev. E **64**, 061901 (2001).

[9] F.C. Larche, J. Appel, G. Porte, P. Bassereau, and J. Marignan, Phys. Rev. Lett. **56**, 1700 (1986).

[10] C.R. Safinya, D. Roux, G.S. Smith, S.K. Sinha, P. Dimon, N.A. Clark, and A.M. Belocq, Phys. Rev. Lett. **57**, 2718 (1986); See also D. Roux and C.R. Safinya, J. Phys. (Paris) **49**, 307 (1988).

[11] L. Golubović and T.C. Lubensky, Phys. Rev. B **39**, 12 110 (1989).

[12] N. Lei, C.R. Safinya, and R.F. Bruinsma, J. Phys. II **5**, 1155 (1995).

[13] R. Holyst, Phys. Rev. A **42**, 7511 (1990); R. Holyst, D.J. Tweet, and L.B. Sorensen, Phys. Rev. Lett. **65**, 2153 (1990).

[14] L.D. Landau and E.M. Lifshitz, *Statistical Physics* (Pergamon, Oxford, 1969).

[15] P.G. de Gennes and J. Prost, *Physics of Liquid Crystals* (Oxford University Press, Oxford, 1993), Chap. 7. For applications of the interface model to the lenticular fractures in smectic-*A* liquid crystals, see P.G. De Gennes, Europhys. Lett. **13**, 709 (1990). For applications to the hairpin turn dislocations in 2D smectic liquid crystals of long semiflexible molecules, see Ref. [8].

[16] G. Grinstein and R.A. Pelcovits, Phys. Rev. Lett. **47**, 856

(1981); Phys. Rev. A **26**, 915 (1982).
[17] W. Helfrich, Z. Naturforsch. Teil A **33**, 305 (1978); W. Helfrich and R.M. Servus, Nuovo Cimento D **3**, 137 (1984).
[18] T. Odijk, Macromolecules **19**, 2313 (1986); D. Roux and C. Coulon, J. Phys. (France) **47**, 1257 (1986).
[19] M. Dijkstra, D. Frenkel, and H.N.W. Lekkerkerker, Physica A **193A**, 374 (1993).
[20] T.W. Burkhardt, J. Phys. A **30**, L167 (1997).
[21] For a review, see *Statistical Mechanics of Membranes and Surfaces*, edited by D.R. Nelson, T. Piran, and S. Weinberg (World Scientific, Singapore, 1989).
[22] G. Gompper and D.M. Kroll, Europhys. Lett. **9**, 59 (1989). For a review, see D. Sornette and N. Ostrowsky, in *Micelles, Membranes, Microemulsion, and Membranes*, edited by W.M. Gelbart, A. Ben-Shaul, and D. Roux (Springer-Verlag, New York, 1994), p. 251.
[23] L. Gao and L. Golubović, Phys. Rev. E **66**, 051918 (2002).
[24] S.-K. Ma, *Modern Theory of Critical Phenomena* (W. A. Benjamin, Inc., Reading, 1976).
[25] L. Golubović and T.C. Lubensky, Phys. Rev. A **41**, 4343 (1990); L. Golubović, Phys. Rev. E **50**, R2419 (1994); D. Morse, *ibid.* **50**, R2423 (1994).
[26] R. Podgornik and V.A. Parsegian, Langmuir **8**, 557 (1992), and therein; H.I. Petrache, N. Gouliaev, S. Tristram-Nagle, R. Zhang, R.M. Suter, and J.F. Nagle, Phys. Rev. E **57**, 7014 (1998).
[27] M. Vogel, C. Münster, W. Fenzl, and T. Salditt, Phys. Rev. Lett. **84**, 390 (2000).